TIM-1 Ubiquitination Mediates Dengue Virus Entry

Ophélie Dejarnac, Mohamed Lamine Hafirassou, Maxime Chazal, Margaux Versapuech, Julien Gaillard, Manuel Perera-Lecoin, Claudia Umana-Diaz, Lucie Bonnet-Madin, Xavier Carnec, Jean-Yves Tinevez, et al.

▶ **To cite this version:**

Ophélie Dejarnac, Mohamed Lamine Hafirassou, Maxime Chazal, Margaux Versapuech, Julien Gaillard, et al.. TIM-1 Ubiquitination Mediates Dengue Virus Entry. Cell Reports, 2018, 23 (6), pp.1779-1793. 10.1016/j.celrep.2018.04.013 . hal-02327431

HAL Id: hal-02327431
https://hal.science/hal-02327431v1

Submitted on 19 Feb 2020

HAL is a multi-disciplinary open access archive for the deposit and dissemination of scientific research documents, whether they are published or not. The documents may come from teaching and research institutions in France or abroad, or from public or private research centers.

L'archive ouverte pluridisciplinaire **HAL**, est destinée au dépôt et à la diffusion de documents scientifiques de niveau recherche, publiés ou non, émanant des établissements d'enseignement et de recherche français ou étrangers, des laboratoires publics ou privés.

Distributed under a Creative Commons Attribution - NonCommercial - NoDerivatives 4.0 International License

Article

Cell Reports

TIM-1 Ubiquitination Mediates Dengue Virus Entry

Graphical Abstract

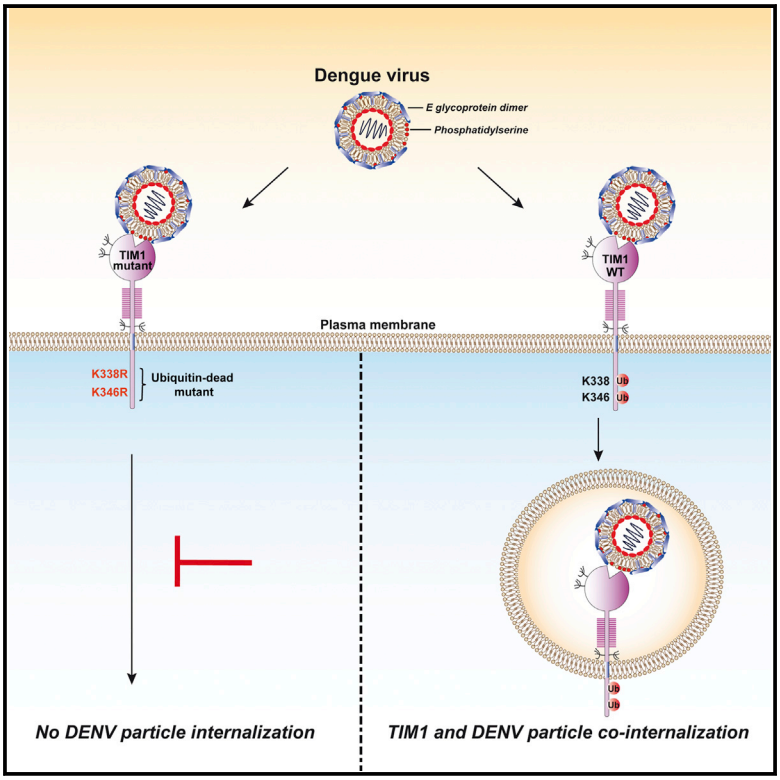

Authors

Ophélie Dejarnac, Mohamed Lamine Hafirassou, Maxime Chazal, ..., Clarisse Berlioz-Torrent, Laurent Meertens, Ali Amara

Correspondence

laurent.meertens@inserm.fr (L.M.), ali.amara@inserm.fr (A.A.)

In Brief

Dejarnac et al. find that the phosphatidylserine receptor TIM-1 is a *bona fide* DENV receptor that mediates virus uptake through the clathrin-mediated pathway. TIM-1 is ubiquitinated at two lysines in its cytoplasmic tail and interacts with STAM-1 for efficient DENV infection.

Highlights

- Genetic ablation of TIM-1 impairs DENV infection
- TIM-1 is an authentic DENV entry receptor
- TIM-1 ubiquitination is important for DENV endocytosis
- STAM-1 interacts with TIM-1 and is required for DENV infection

Dejarnac et al., 2018, Cell Reports *23*, 1779–1793
May 8, 2018 © 2018 The Author(s).
https://doi.org/10.1016/j.celrep.2018.04.013

CellPress

Cell Reports
Article

OPEN ACCESS
CellPress

TIM-1 Ubiquitination Mediates Dengue Virus Entry

Ophélie Dejarnac,[1,8] Mohamed Lamine Hafirassou,[1,8] Maxime Chazal,[2] Margaux Versapuech,[3] Julien Gaillard,[4] Manuel Perera-Lecoin,[1] Claudia Umana-Diaz,[1] Lucie Bonnet-Madin,[1] Xavier Carnec,[1] Jean-Yves Tinevez,[5] Constance Delaugerre,[6] Olivier Schwartz,[7] Philippe Roingeard,[4] Nolwenn Jouvenet,[2] Clarisse Berlioz-Torrent,[3] Laurent Meertens,[1,*] and Ali Amara[1,9,*]

[1]INSERM U944-CNRS 7212, Laboratoire de Pathologie et Virologie Moléculaire, Institut Universitaire d'Hématologie, Université Paris Diderot Sorbonne Paris Cité, Hôpital St. Louis, 75475 Paris Cedex 10, France
[2]Viral Genomics and Vaccination Unit, UMR-3569 CNRS, Pasteur Institute, 75724 Paris, France
[3]Laboratoire Interaction Hôte-Virus, Institut Cochin, INSERM U1016-CNRS UMR8104-Université Paris Descartes, 75014 Paris, France
[4]INSERM U966 MAVIVH, Faculté de Médecine, Université de Tours, Tours, France
[5]Institut Pasteur, Citech, UTechS PBI, 75724 Paris Cedex 15, France
[6]Departement des Maladies Infectieuses, Hôpital Saint Louis, 75010 Paris, France
[7]Unité Virus et Immunité, Institut Pasteur, 75724 Paris, France
[8]These authors contributed equally
[9]Lead Contact
*Correspondence: laurent.meertens@inserm.fr (L.M.), ali.amara@inserm.fr (A.A.)
https://doi.org/10.1016/j.celrep.2018.04.013

SUMMARY

Dengue virus (DENV) is a major human pathogen causing millions of infections yearly. Despite intensive investigations, a DENV receptor that directly participates in virus internalization has not yet been characterized. Here, we report that the phosphatidylserine receptor TIM-1 is an authentic DENV entry receptor that plays an active role in virus endocytosis. Genetic ablation of TIM-1 strongly impaired DENV infection. Total internal reflection fluorescence microscopy analyses of live infected cells show that TIM-1 is mostly confined in clathrin-coated pits and is co-internalized with DENV during viral entry. TIM-1 is ubiquitinated at two lysine residues of its cytoplasmic domain, and this modification is required for DENV endocytosis. Furthermore, STAM-1, a component of the ESCRT-0 complex involved in intracellular trafficking of ubiquitinated cargos, interacts with TIM-1 and is required for DENV infection. Overall, our results show that TIM-1 is the first *bona fide* receptor identified for DENV.

INTRODUCTION

Dengue is the most common mosquito-borne viral disease caused by one of the four serotypes of dengue virus (DENV-1 to DENV-4). Almost half of the world population is at risk of infection, and about 100 million new infections occur each year (Bhatt et al., 2013). DENV infection causes pathologies ranging from a self-limiting illness called dengue fever (DF) to the life-threatening forms of dengue hemorrhagic fever (DHF) and dengue shock syndrome (DSS) (Guzman and Harris, 2015). To date, there is no specific treatment against DENV infection, and an efficient human vaccine is not available.

DENV enters target cells by receptor-mediated endocytosis. Live-imaging studies have shown that DENV particles bind still uncharacterized cellular receptor(s) and move along the cell surface before being captured by preexisting clathrin-coated pits (CCPs) for uptake by the endocytic machinery (van der Schaar et al., 2007, 2008). The envelope glycoprotein (E protein), organized in 90 homodimers at the surface of DENV particles (Kuhn et al., 2002), mediates virus attachment to cells and fusion of viral and endosomal membranes. When internalized, the low endosomal pH primes E protein for viral fusion without the need for additional host factors (Stiasny et al., 2011). Despite intensive investigations, an authentic receptor that binds virions, participates in virus endocytosis, and triggers infection has not been identified. A few molecules, such as heparan sulfate aminoglycans (Chen et al., 1997) or the C-type lectin DC-SIGN (Navarro-Sanchez et al., 2003; Tassaneetrithep et al., 2003), interact with the DENV E protein and enhance infection (Perera-Lecoin et al., 2013). These molecules are not directly involved in the DENV entry program but mainly work as attachment factors, likely concentrating viral particles at the vicinity of entry receptor(s) (Lozach et al., 2005; Navarro-Sanchez et al., 2003; Tassaneetrithep et al., 2003).

We have previously shown that DENV binding is independent of interactions between E protein and target cells (Carnec et al., 2015; Meertens et al., 2012). It involves the recognition of phospholipids exposed at the surface of DENV by specific "eat me" receptors expressed on target cells. T cell immunoglobulin mucin (TIM-1 and TIM-4) and the TAM (Tyro3 and Axl) receptor families, along with CD300a, are the main receptors that mediate DENV infectious entry (Carnec et al., 2015; Meertens et al., 2012). Their natural function is to interact with phosphatidylserine (PS) or phosphatidylethanolamine (PE) exposed on apoptotic cells to promote their phagocytosis (Kobayashi et al., 2007; Lemke and Rothlin, 2008; Leventis and Grinstein, 2010; Simhadri et al., 2012). DENV hijacks this process for entry and mimics apoptotic cell bodies by exposing PS and PE at the viral membrane (Carnec et al., 2015; Meertens et al., 2012). This

This is an open access article under the CC BY-NC-ND license (http://creativecommons.org/licenses/by-nc-nd/4.0/).

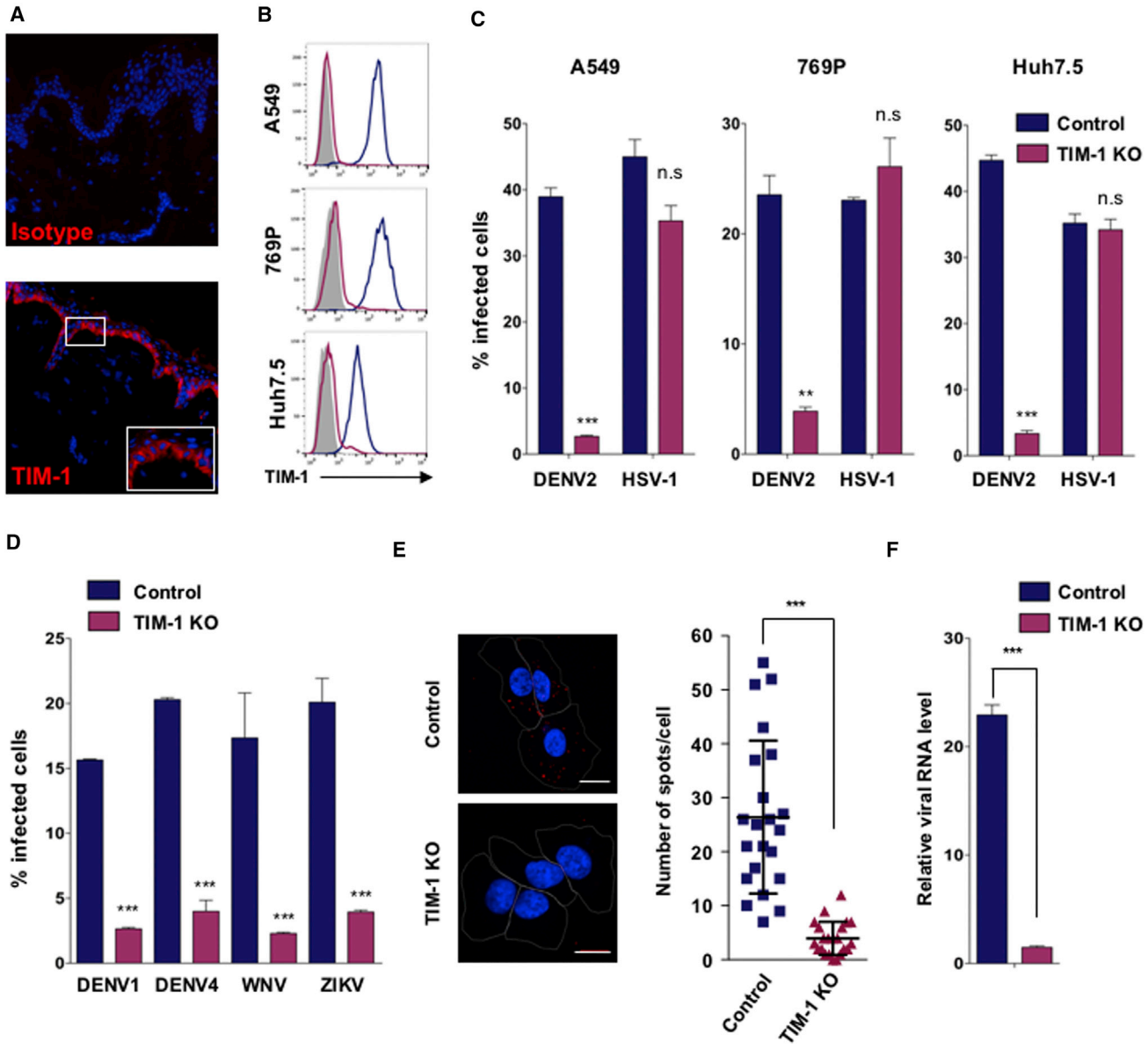

Figure 1. Genetic Ablation of TIM-1 Inhibits DENV Infection

(A) TIM-1 expression in human skin.

(B) TIM-1 cell surface expression in TIM-1 KO cells (red line). Gray shading represents cell staining with a control antibody and the blue line TIM-1 expression in control cells.

(C) Control and TIM-1 KO cell lines were challenged with DENV2 JAM (MOI 1) or HSV-1 (MOI 0.2).

(D) A549 CRISPR control and TIM-1 KO cells were challenged with DENV1, DENV4, WNV, or ZIKV. The levels of infected cells were assessed 24 hours post infection (hpi) by flow cytometry using the respective anti-viral antibodies. Data shown are means ± SD of two independent experiments in duplicate.

(E) A549 control and TIM-1 KO cells were incubated on ice with DENV2 JAM at an MOI of 50. Cells were then stained for DENV viral RNA (red). White lines outline the cell membrane. Data shown on the left are representative of two independent experiments. Scale bar, 20 μm. Right: quantification of DENV RNA spots counted per cells for each condition (n > 20).

(F) A549 TIM-1 KO and control cells were incubated with DENV2 JAM for 1 hr at 4°C and shifted to 37°C for 2 hr. Cells were then treated with proteinase K (1 mg/mL) for 45 min at 4°C, total RNA was extracted, and relative viral RNA was quantified by qRT-PCR. Data shown are representative of two independent experiments.

Significance was calculated using a two-sample Student's t test (D, F, and G) or a one-way ANOVA statistical test with a Tukey post-test (E). n.s., non-significant; **$p < 0.001$; ***$p < 0.0001$.

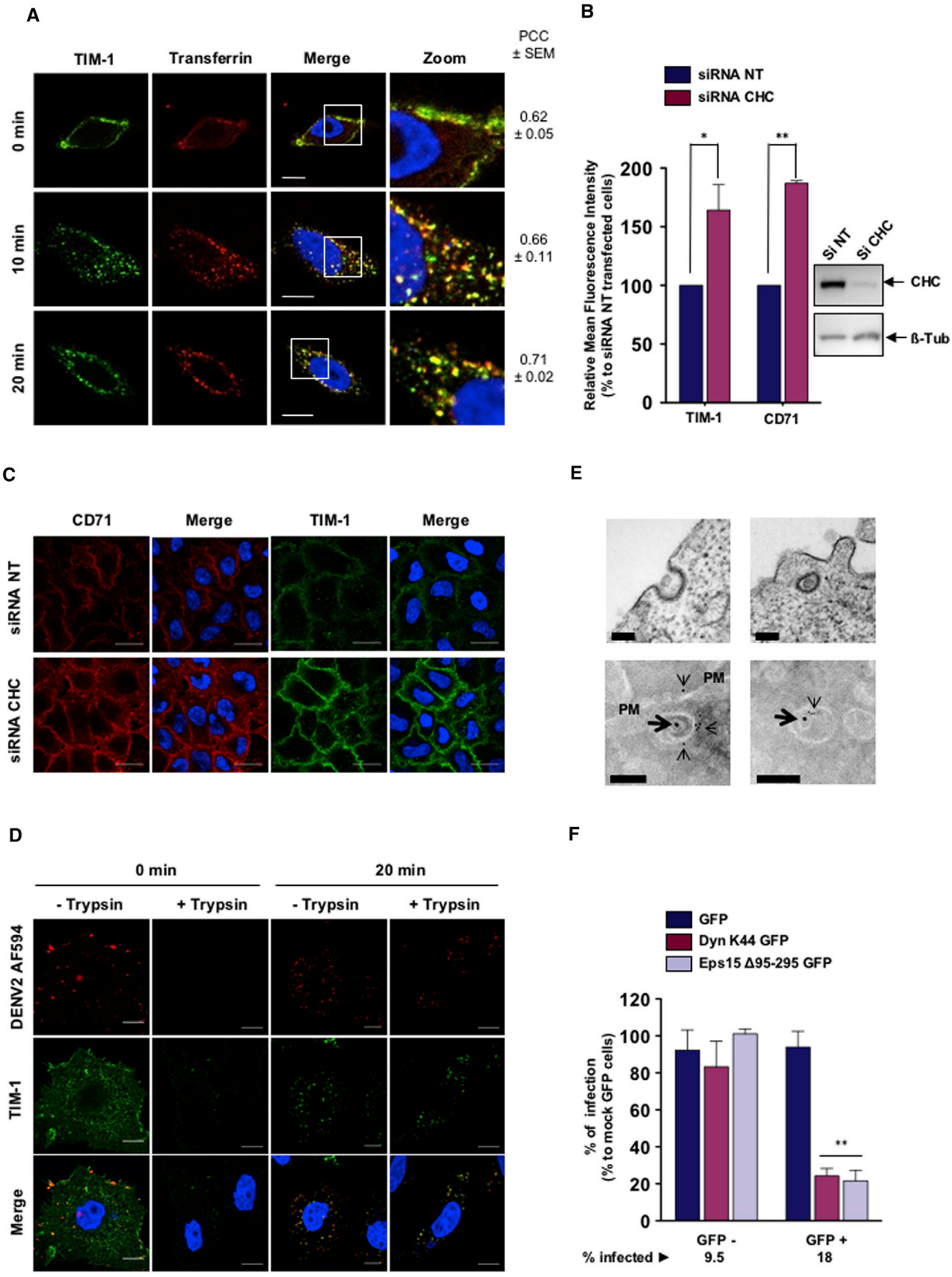

(legend on next page)

viral apoptotic mimicry strategy may be exploited by flaviviruses and other viruses, probably to broaden viral tropism and escape innate immunity (Amara and Mercer, 2015; Bhattacharyya et al., 2013; Hamel et al., 2015; Jemielity et al., 2013; Kondratowicz et al., 2011; Meertens et al., 2017; Mercer and Helenius, 2008; Moller-Tank et al., 2013; Morizono and Chen, 2014; Shimojima et al., 2006; Vanlandschoot and Leroux-Roels, 2003).

TIM-1 is a type I transmembrane glycoprotein with an extracellular domain composed of an N-terminal immunoglobulin V (IgV)-like domain followed by a glycosylated mucin domain, a transmembrane domain, and a short cytoplasmic tail (Freeman et al., 2010). A conserved cavity within the IgV-like domain, called the metal ion-dependent ligand-binding site (MILIBS), is the binding site for PS (Kobayashi et al., 2007; Santiago et al., 2007). TIM-1 enhances infection by the four DENV serotypes and related flaviviruses (Hamel et al., 2015; Meertens et al., 2017). TIM-1 expression correlates with cell permissiveness to DENV infection (Meertens et al., 2012). DENV infection of permissive cells is inhibited by anti-TIM-1 antibodies or by silencing expression of this receptor with RNAi (Meertens et al., 2012). TIM-1 interacts directly with DENV particles, and mutations of highly conserved amino acids (TIM-1 N114A or D115A and TIM-4 N121A) lining the MILIBS abolish infection (Meertens et al., 2012). Moreover, annexin V, which binds PS, inhibits TIM-mediated enhancement of infection (Meertens et al., 2012). TIM-1 enhances DENV internalization (Meertens et al., 2012) through mechanisms that are not characterized. TIM-1 is constitutively internalized by clathrin-mediated endocytosis (Balasubramanian et al., 2012), the major DENV entry route (Acosta et al., 2008, 2009; van der Schaar et al., 2008). One important question concerning TIM-1 is whether this molecule serves as an authentic DENV endocytic receptor or whether it only enhances virus attachment.

Here we have studied the molecular mechanisms of TIM-1-mediated DENV infection in several cellular models. We show that TIM-1 plays an active role in viral endocytosis and that it is the first *bona fide* entry receptor identified for DENV.

RESULTS AND DISCUSSION

TIM-1 Is an Important Cellular Receptor for DENV Infection

To study the role of TIM-1 in DENV infection, we first examined its localization in human skin, the entry site of the virus during the mosquito bite. TIM-1 is expressed on human keratinocytes located at basal layer of the skin epidermis and is not detected in other regions (Figure 1A). Gain-of-function studies showed that ectopic TIM-1 expression in several non-permissive cells confers DENV infection (Figure S1). To prove that endogenous TIM-1 molecules are important for DENV infection, we generated TIM-1 knockout A549, Huh7.5, and 769P cells by CRISPR/Cas9 (Figure 1B). DENV2 infection was significantly inhibited in cells lacking TIM-1 (Figure 1C), whereas herpes simplex virus 1 (HSV-1) infection was not affected. TIM-1 was also required for productive infection of A549 cells by other DENV serotypes, West Nile virus (WNV) and Zika virus (ZIKV) (Figure 1D). We then performed a fluorescence *in situ* hybridization (FISH) assay to detect virus binding at the cell surface (Figure 1E). TIM-1 plays an essential role in DENV capture because very little viral RNA (vRNA) was detected in Huh7.5 TIM-1 knockout (KO) cells compared with control cells. Consistently, the amount of internalized DENV RNA was significantly reduced in TIM-1 KO cells compared with control cells (Figure 1F). Altogether, these data show that TIM-1 promotes DENV binding and infection in various human cell lines. Of note, residual viral binding and infection were observed in TIM-1 KO cells, suggesting that TIM-1 is the main but not the only receptor for DENV.

TIM-1 and DENV Are Co-internalized during Virus Entry

To investigate TIM-1 trafficking in human cells, we performed immunofluorescence staining of TIM-1 and AF594-conjugated transferrin (Tf) in different cell types (Figure S2A). Consistent with a previous study (Balasubramanian et al., 2012), confocal microscopy studies showed that a large proportion of TIM-1 molecules exist in intracellular pools that co-localize with Tf. This suggests that TIM-1 is constitutively internalized through clathrin-mediated endocytosis (CME), the major DENV entry

Figure 2. TIM-1 and DENV Co-internalized through CME

(A) Confocal microscopy analysis of TIM-1 and transferrin internalization. HeLa TIM-1 cells were incubated with transferrin-AF594 and mouse anti-TM-1 primary antibody for 1 hr at 4°C and shifted to 37°C. At the indicated time points, cells were fixed, permeabilized, and immunostained with a goat anti-mouse Alexa 488-conjugated secondary antibody. Scale bars, 10 μm. Pearson correlation coefficients (PCCs) were calculated using ImageJ software (n = 5). Images are representative of at least three independent experiments.

(B and C) HeLa TIM-1-expressing cells were transfected with a siRNA pool targeting clathrin heavy chain (CHC) or a non-targeting (NT) siRNA pool. Cell surface expression of TIM-1 and CD71 was assessed 48 hr after transfection by flow cytometry (B) or by confocal microscopy (C) under non-permeabilized conditions. Data shown are means ± SD of two independent experiments.

(D) Confocal microscopy analysis of TIM-1 and DENV2 internalization. HeLa parental or TIM-1-expressing cells were incubated with DENV2 AF594 and mouse anti-TIM-1 primary antibody for 1 hr at 4°C and shifted to 37°C. At the indicated time points, cells were treated or not treated with trypsin, permeabilized, and immunostained with a goat anti-mouse Alexa 488-conjugated secondary antibody. Scale bars, 10 μm. Images are representative of at least three independent experiments.

(E) Transmission electron microscopy and immunogold labeling of TIM-1 and DENV particles in infected cells. Top: images obtained by standard transmission electron microscopy, showing endocytosis of DENV particles mediated by clathrin-coated vesicles (scale bars, 100 nm). Bottom: immunogold labeling of TIM1 (6-nm gold particles, small arrows) and DENV-E (10-nm gold particles, large arrows) in cryosections. TIM-1 is localized at the membrane of clathrin-coated vesicles containing DENV particles. PM, plasma membrane. Scale bars, 100 nm.

(F) TIM-1-expressing cells were transfected with dominant-negative (DN) forms of EGFP-dynamin (Dyn K44) and -Eps15 (Eps15 Δ95-215) or with the respective GFP control plasmids. Cells were challenged with DENV2 JAM 24 hr after transfection. For each sample, infection was quantified by flow cytometry in the GFP-positive population. Data shown are means ± SD of two independent experiments.

For (B) and (E), significance was calculated using one-way ANOVA statistical test with Tukey post-test (*$p < 0.01$, **$p < 0.001$.

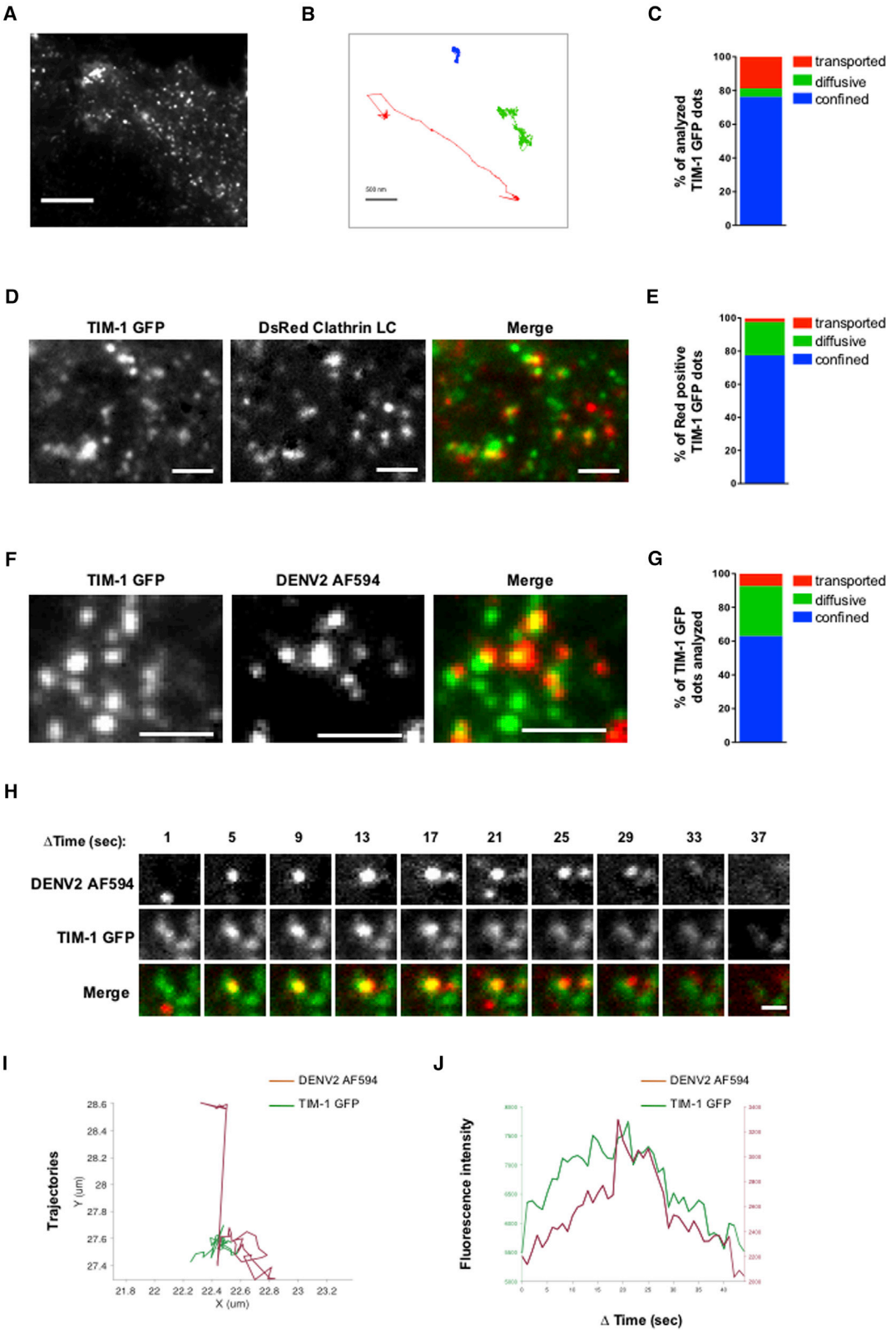

(legend on next page)

route for productive infection (Acosta et al., 2008; van der Schaar et al., 2008). To study the kinetics of TIM-1 internalization from the cell surface, HeLa TIM-1 cells were co-incubated with saturating concentrations of a non-neutralizing anti-TIM-1 monoclonal antibody (mAb) and AF594-Tf for 1 hr at 4°C. Cells were either kept on ice (0 min) or shifted at 37°C to allow endocytosis and then analyzed at various time points. Internalized TIM-1/anti-TIM-1 complexes were detected using a fluorescent secondary antibody (Ab) under permeabilized conditions. At 0 min, TIM-1/anti-TIM complexes were mainly detected at the cell surface (Figure 2A). Upon internalization, the majority of TIM-1 receptor co-localized with Tf (Figure 2A). To confirm that TIM-1 traffics through CME, the expression of clathrin heavy chain (CHC) was knocked down using RNAi. Under these conditions, TIM-1 accumulated at the cell surface, similar to the CD71 Tf receptor, which is known to be internalized via CME (Figures 2B and 2C).

We then studied TIM-1 and DENV localization in fixed cells using confocal microscopy. We generated Alexa Fluor 594-labeled DENV2 particles (DENV2 AF594). DENV labeling did not affect infectivity (Figure S2B) or binding to TIM-1 (Figure S2C). Inside-out staining experiments showed that the vast majority of TIM-1 Abs co-localized with DENV2 AF594 during viral entry (Figure 2D), strongly suggesting that they are co-internalized. Electron microscopy studies supported these finding and showed that, in TIM-1-positive cells, DENV enters via CME (Figure 2E). Furthermore, both the virus and receptor trafficked together during endocytosis and were located in the same endosomal compartments (Figures 2D and 2E; Figure S2D). TIM-1-mediated DENV infection was abrogated in HeLa TIM-1 cells knocked down for CHC expression (Figure S2E) or by ectopically expressing the dominant-negative (DN) forms of Eps15 and Dynamin, two cellular proteins essential for CME (Figure 2F). Therefore, TIM-1 mediates DENV endocytosis and is co-internalized with viral particles through CME.

Dynamics of TIM-1-Mediated DENV Internalization

To study the dynamics of TIM-1 at the plasma membrane, total internal reflection fluorescence (TIRF) microscopy experiments were performed in live cells. TIRF microscopy generates an evanescent field that penetrates ~100 nm deep into cells; therefore, only cell surface molecules are excited by the laser and can emit a fluorescent signal. This approach is particularly well suited to analyze the localization and the dynamics of molecules and events near the plasma membrane in living cells (Poulter et al., 2015). We generated a HeLa cell line that stably expresses TIM-1 fused to the GFP. TIM-1 GFP protein exhibited a similar cellular localization as the wild-type (WT) receptor and enhanced DENV infection with similar efficiency (Figures S3A and S3B). TIRF microscopy analysis showed that TIM-1 GFP puncta displayed distinct dynamic dots at the plasma membrane (Figure 3A). Using TrackMate and MATLAB software, we analyzed 7400 TIM-1 GFP spots trajectories from 10 cells. TIM-1 exhibited three different types of motions at the cell surface (Figure 3B). Although the majority of TIM-1 stayed confined within a limited area of the plasma membrane (76%), the remaining portion was either transported across the cell surface (19%) or diffusive at the plasma membrane (5%) (Figures 3B and 3C). Because TIM-1 internalizes through CME, we determined whether these confined TIM-1 molecules were associated with CCPs. TIRF studies performed with TIM-1 GFP cells transiently expressing dsRed-clathrin light chain (CLC) (Figure 3D) showed that the majority of TIM-1 spots that co-localized with CLC displayed a confined displacement (Figure 3E). These data strongly suggest that TIM-1 is mostly confined in CCPs at the plasma membrane. To record virus internalization in live cells, dual-color TIRF images were acquired at 37°C immediately after DENV2 AF594 addition to the culture medium of HeLa TIM-1 GFP cells. The small size of DENV particles (50–60 nm in diameter) allowed virus diffusion into the narrow space between the cell and the coverslip. The dynamic of viruses bound to the bottom of the cells was thus accessible via TIRF imaging (Figure 3F). Robust individual viral particle tracking requires high-speed imaging and low particle density. We therefore exposed cells to DENV2 AF594 at an MOI of 1 and immediately acquired images every second for 20–40 min. The dynamics of 27 DENV particles (in 8 cells) that associated with TIM-1 GFP were recorded. The majority of TIM-1 GFP dots tracked for DENV2 internalization displayed confined displacement at the plasma membrane (Figure 3G). The trajectories of these 27 events were analyzed (Figure S3C), and one representative track is shown in Figure 3H. In 6 cases, DENV particles exhibited lateral movements in the TIRF field, followed by confined movement when associated with TIM-1 (Figure 3I). Such behavior suggests that DENV may interact with another attachment factor before binding to TIM-1. In 16 cases, DENV2 AF594 and TIM-1 GFP trajectories perfectly overlapped from the beginning of acquisition to the disappearance of the DENV-TIM-1 complexes from the field. In 5 of these recordings, both DENV and TIM-1 exhibited lateral movements

Figure 3. Live Imaging of TIM-1 and DENV AF594 Co-Internalization by TIRF Microscopy

(A) TIRF image of HeLa cells stably expressing TIM-1 GFP. Scale bar, 10 μm.

(B) Motility and trajectory analysis of the TIM-1-GFP receptor at the plasma membrane. Analysis was done on 9 different TIRF microscopy videos and a total of 7,490 tracks. 76.2% of spots were found to be confined (blue), 5.0% diffusive (green), and 18.9% transported (red). Scale bar, 500 nm.

(C) Representative graph of TIM-1 GFP mobility at the plasma membrane.

(D) HeLa TIM-1 GFP (green) cells were transfected with clathrin light chain-dsRed (clathrin LC-DsRed, red) 48 hr before live imaging by TIRF microscopy. Scale bar, 2 μm.

(E) Representative graph of TIM-1 GFP movement when found co-localized with clathrin LC-dsRed (Red positive). Data are representative of the percentage of total spots tracked (n = 120).

(F) HeLa TIM-1 GFP cells were imaged by TIRF microscopy in the continuous presence of DENV2 AF594. Scale bar, 2 μm.

(G) Distribution of tracked TIM-1 spots that co-localized and internalized DENV2 AF594. Data are representative of the percentage of total spots tracked (n = 27).

(H) Time-lapse series images of TIM-1-GFP (green) and DENV2 AF594 (red) simultaneously disappearing from the TIRF field. Scale bar, 0.5 μm.

(I) Magnification of TIM-1-GFP (green) and DENV2 AF594 (red) trajectories obtained from the spots tracked in (H).

(J) Respective average fluorescence intensity of TIM-1-GFP (green) and DENV2 AF594 (red) over time from the spot tracked in (H).

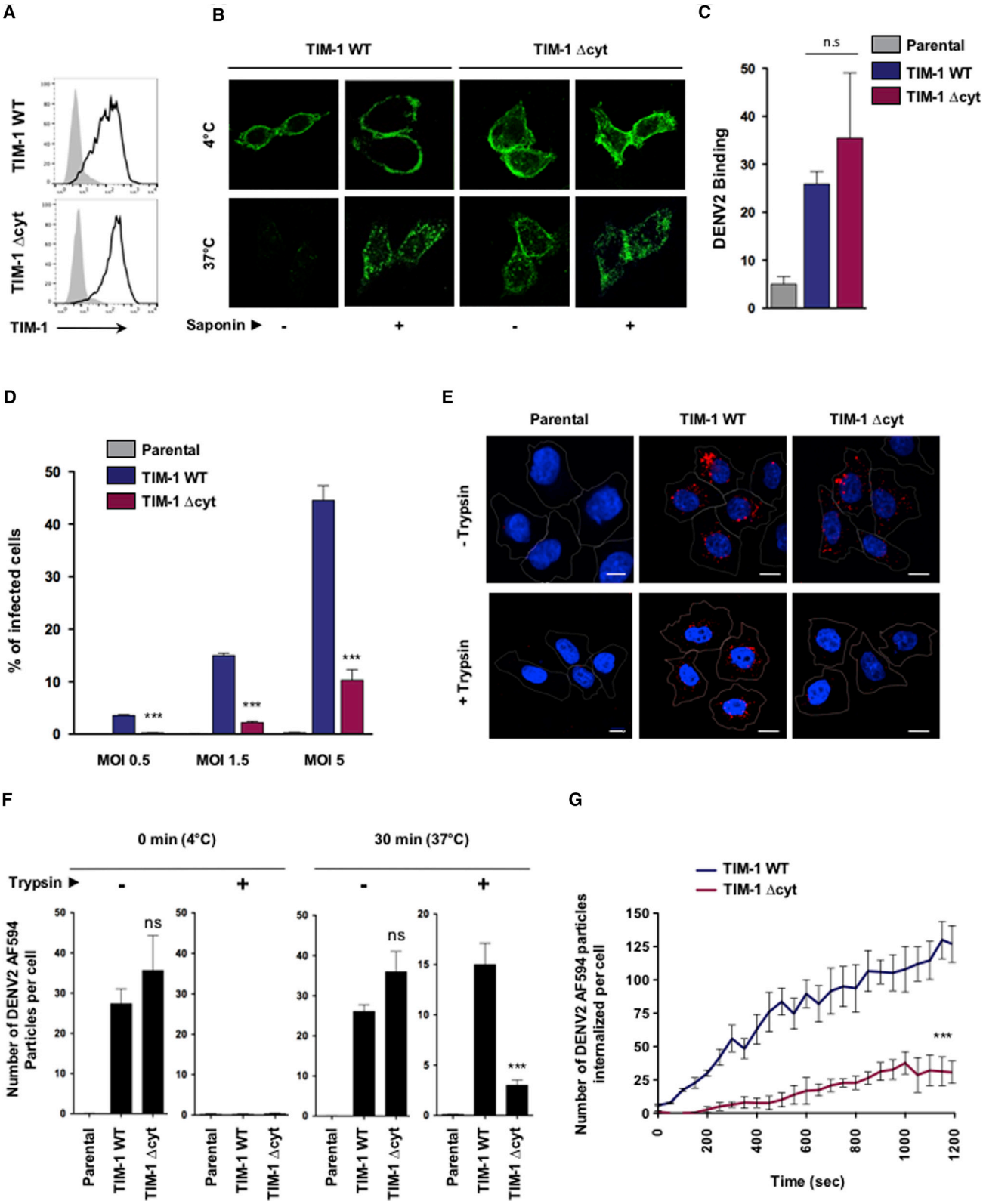

(legend on next page)

within the plasma membrane, and then a confined trajectory occurred when they associated (Figure S3C). The mean fluorescence intensities corresponding to DENV2 AF594 (red) and TIM-1 GFP (green) were also measured over time (Figure 3J). The fluorescence intensities of the two signals decreased in parallel, suggesting concomitant internalization of DENV2 AF594 and TIM-1 GFP from the plasma membrane. These data also suggest that the interaction between DENV2 AF594 and TIM-1 GFP may be long-lasting and/or very strong; when the virus and TIM-1 GFP are associated, they remained bound until both signals simultaneously disappear from the field (Figure 3J). On average, DENV particles stayed in the TIRF field for about 40 s (with variation from 8 to 150 s). Together, TIRF microscopy analyses further demonstrate that TIM-1 and DENV particles interact at the plasma membrane and suggest that this interaction most likely drives virus internalization.

The TIM-1 Cytoplasmic Domain Is Important for DENV Internalization

TIM-1 promotes DENV internalization; however, the exact molecular and cellular mechanisms involved are unknown. To investigate whether the TIM-1 cytoplasmic domain is required for endocytosis, we generated HeLa cells stably expressing TIM-1 lacking this domain (TIM-1 Δcyt) (Figure 4A). Cells were incubated with anti-TIM-1 Abs, shifted at 37°C for 20 min, and then permeabilized or not with saponin to discriminate surface from internalized TIM-1 receptors (Figure 4B). At 4°C, both TIM-1 WT and TIM-1 Δcyt were localized at the plasma membrane. When cells were incubated at 37°C, the WT molecule was efficiently internalized, whereas TIM-1 Δcyt mainly remained at the cell surface (Figures 4B and S4A). The cytoplasmic domain of TIM-1 is thus required for TIM-1 constitutive endocytosis. We previously showed that DENV infection is modestly reduced in HEK293T cells overexpressing the TIM-1 Δcyt mutant (Meertens et al., 2012). We confirmed these results in cells that stably express this molecule. The TIM-1 Δcyt mutant bound DENV particles with similar efficiency as its WT counterpart (Figure 4C). DENV2 infection was strongly impaired in cells expressing TIM-1 Δcyt, whatever the MOI tested (Figure 4D). Similar results were obtained with another DENV serotype (DENV3 THAI) in HEK293T cells expressing TIM-1 WT or the Δcyt mutant (Figures S4B and S4C). To investigate the ability of the TIM-1 Δcyt mutant to promote DENV endocytosis, we visualized and quantified viral internalization using multiple methods. First, we incubated parental, TIM-1 WT, or TIM-1 Δcyt-expressing cells with DENV2 at 4°C to synchronize viral binding and then shifted them to 37°C for 30 min to allow viral internalization. Cells were then treated with trypsin to eliminate viral particles remaining at the cell surface, and vRNA was detected by FISH (Figure 4E). In a second approach, we incubated parental and TIM-1-expressing cells with DENV2 AF594 and quantified virus binding and endocytosis using Fiji software. As expected, TIM-1 WT and TIM-1 Δcyt similarly bound DENV2 AF594 particles (Figure 4F, 0 min (4°C) –trypsin). Trypsin removed the signal at the cell surface (Figure 4F, 0 min (4°C) +trypsin). However, after 30 min at 37°C, TIM-1 Δcyt cells showed a strong defect in viral particle internalization compared with TIM-1 WT cells (Figures 4F and S4D). We then recorded DENV2 AF594 internalization in live cells using spinning disk confocal microscopy. Using Fiji and TrackMate, we quantified the number of internalized DENV2 AF594 particles every 2 s for up to 20 min (Figure 4G, red dots). This assay also indicated that the cytoplasmic tail of TIM-1 is important for DENV endocytosis. Interestingly, TIM-1 Δcyt mediated internalization of apoptotic thymocytes, similar to TIM-1 WT or a TIM mutant expressing a GPI anchor (Figures S4E–S4G). Taken together, these data show that the TIM-1 cytoplasmic domain is essential for DENV endocytosis but not for phagocytosis of apoptotic cells.

TIM-1 Ubiquitination Regulates DENV Endocytosis

The TIM-1 cytoplasmic tail does not contain any canonical endocytic domains such as di-leucine or tyrosine-based motifs. We noticed the presence of two lysines (K338 and K346) located in the TIM-1 cytoplasmic region that may act as ubiquitination sites (Figure 5A). Ubiquitin (Ub) is a post-translational modification reported to promote receptor endocytosis and target receptors for lysosomal degradation and termination of receptor signaling (Haglund and Dikic, 2012; Shih et al., 2000). To investigate whether TIM-1 is ubiquitinated, we generated HeLa cells expressing mutants of the cytoplasmic tail of TIM-1 in which single or both lysine residues at position 338 and 346 were substituted with arginines ($K_{338}R$, $K_{346}R$, and KKRR) (Figure 5B).

Figure 4. The TIM-1 Cytoplasmic Domain Is Essential for TIM-1-Mediated DENV Infection and Internalization

(A) Surface expression of TIM-1 in HeLa cells stably expressing WT or Δcyt mutant TIM-1.

(B) Confocal microscopy of TIM-1 WT and Δcyt mutant endocytosis. Cells were incubated with primary mouse anti-TIM-1 antibody (30 μg/mL) for 1 hr at 4°C and shifted to 37°C for 20 min. Cells were fixed and stained with secondary goat anti-mouse Alexa 488-conjugated antibody in the presence or absence of saponin. Images are representative of at least three independent experiments.

(C) DENV2 binding quantification by qRT-PCR on parental, TIM-1 WT, or Δcyt-expressing HeLa cells. Cells were incubated with DENV2 JAM for 1 hr on ice and washed extensively. Total RNA was extracted, and relative viral RNA was quantified by qRT-PCR. Data shown are means ± SD of two independent experiments.

(D) DENV2 infection of parental, TIM-1 WT, and TIM-1 Δcyt mutant HeLa cells. Cells were challenged with DENV2 JAM at the indicated MOI, and the level of infection was assessed 24 hpi by flow cytometry. Data are shown as mean ± SD of at least three independent experiments.

(E) Parental, TIM-1 WT, or TIM-1 Δcyt-expressing HeLa cells were incubated on ice with DENV2 JAM at a MOI of 50. Cells were shifted at 37°C for 60 min and treated or not treated with trypsin for 15 min at 4°C. Cells were then fixed, permeabilized, and stained for DENV viral RNA (red). White lines outline the cell membrane. Scale bars, 10 μm. Images are representative of three independent experiments.

(F) Parental, TIM-1 WT, or Δcyt-expressing HeLa cells were incubated with DENV2 AF594 for 1 hr on ice and then shifted to 37°C for 30 min or kept at 4°C as a control. Cells were treated with trypsin to remove cell surface-bound DENV2 AF594 particles. DENV2 AF594 particles were quantified by immunofluorescence using Fiji software. Data are shown as mean ± SD of at least three independent experiments (n > 150 cells for each condition).

(G) Quantification of DENV2 AF594 particles internalized in live HeLa TIM-1 WT or HeLa TIM-1Δcyt cells over time. Quantification was done from videos recorded by spinning disk live microscopy (n = 3). Data are shown as mean ± SD for each time point.

Significance was calculated using one-way ANOVA (C, D, and F) or a two-sample Student's t test (G); ***$p < 0.0001$.

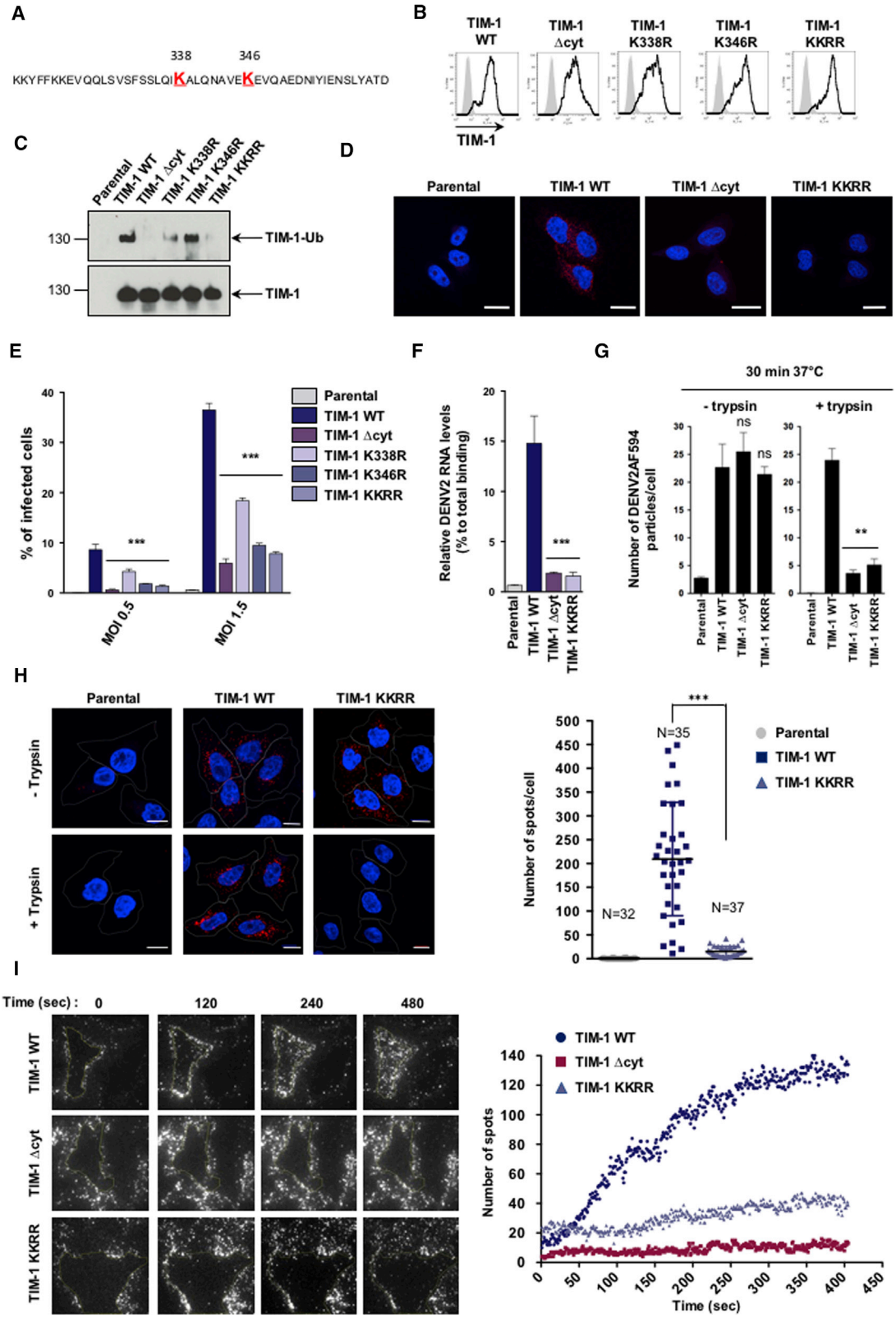

(legend on next page)

We immunoprecipitated these proteins to assess their ubiquitination status. Immunoblot analysis using a FK2 Ab, which recognizes mono- and polyubiquitinated proteins, showed that both the K338 and K346 residues are required for TIM-1 ubiquitination (Figure 5C). A proximity ligation assay (PLA) using anti-TIM-1 and FK2 Abs allowed visualization of the association of Ub with the WT molecule but not with Δcyt and KKRR TIM-1 (Figure 5D). Therefore, the two K_{338} and K_{346} residues are essential for TIM-1 ubiquitination. We then challenged cells expressing TIM-1 mutants with DENV2 JAM and quantified viral infection by flow cytometry (Figure 5C). TIM-1 K_{338}R promoted DENV2 infection less efficiently than TIM-1 WT. The TIM-1 K_{346}R and KKRR double mutants were even more impaired (Figure 5E). To analyze whether TIM-1 ubiquitination affects DENV internalization, we quantified, by qRT-PCR, the levels of vRNA internalized after 2 hr at 37°C. The mutant TIM-1 KKRR internalized significantly fewer viral particles than the WT molecule (Figure 5F). TIM-1 WT and mutant-expressing cells bound DENV2 AF594 particles with similar efficiency (Figure S5A). Trypsin treatment removed cell surface-bound viral particles at 4°C (Figure S5A). After 30 min at 37°C, viral particles were mostly detected only in HeLa cells expressing TIM-1 WT, whereas TIM-1 Δcyt and TIM-1 KKRR mutants internalized significantly fewer viral particles (Figure 5G; Figure S5A). We further confirmed these results using vRNA detection by FISH. Quantification of internalized DENV RNA dots (red) demonstrated that vRNA was significantly less endocytosed in cells expressing the KKRR mutant compared with TIM-1 WT (Figure 5H). Of note, we observed that the TIM-1 Ub profile was unaffected by DENV during entry (Figure S5B). We then analyzed, by TIRF microscopy, the motility of DENV2 AF594 at the plasma membrane in TIM-1 WT, Δcyt-, or KKRR-expressing cells (Figure 5I). With TIM-1 WT, viruses were first observed at the edge of the cell (Figure S5C). After 5–6 min, the entire cell surface was covered with viruses, suggesting that they were diffusing laterally prior to endocytosis. By contrast, no lateral transport was observed in the presence of TIM-1 mutants (Figure 5I; Figure S5C). Consistent with these data, electron microscopy studies indicated that TIM-1 WT is expressed at the cell membrane and also detected in multivesicular bodies (MVBs), whereas the TIM-1 KKRR mutant was mainly detected at the plasma membrane (Figure S5C). Together, these data indicate that TIM-1 ubiquitination regulates DENV lateral motility at the cell surface, internalization, and productive infection.

Proteomics Analysis of TIM-1 Cellular Partners Identifies STAM as a Host Factor for DENV Infection

To uncover the host factors that associated with TIM-1 during DENV internalization, we generated HeLa cells stably expressing a molecule carrying a double FLAG and hemagglutinin (HA) tag at the end of the cytoplasmic tail (TIM-1 FLAG-HA; Figure S6A). This tagged form of TIM-1 enhanced DENV infection as efficiently as TIM-1 WT (Figure S6B). HeLa cells expressing TIM-1 WT or TIM-1 FLAG-HA were then differentially labeled with stable isotope labeling with amino acids (SILAC) and lysed. The two lysates were pooled equally, and two successive immunoprecipitations using beads coupled with anti-FLAG M2- and anti-HA-specific IgG were used to purify TIM-1 FLAG-HA (Figure S6C). Co-precipitated proteins were purified by SDS-PAGE (Figure S6D) and analyzed by mass spectrometry. We defined a threshold > 2 according to the isotope ratio $^{13}C/^{12}C$ (Table 1). Above this threshold, we identified 22 host proteins (Table 1). Among them, FYN, a previously known TIM-1 binding partner (Curtiss et al., 2011), was detected, validating our approach. We then analyzed the protein-protein interaction network of the identified TIM-1 binding factors using the STRING database (Figure S6E). This analysis highlighted an important network of proteins implicated in the regulation of protein ubiquitination, including four E3 Ub ligases (ITCH, RNF149, STUB1, and NEDD4L), receptor trafficking, and endosomal sorting proteins (Table 1; Figure S6E). We then performed a loss-of-function screening to determine the effect of each factor in DENV

Figure 5. Ubiquitination of the TIM-1 Cytoplasmic Domain Is Required for DENV Infection and Internalization

(A) Amino acid sequence of the TIM-1 cytoplasmic domain. The two mutated lysine residues are indicated in bold red letters.

(B) Cell surface expression of the TIM-1 receptor in TIM-1 WT, TIM-1 Δcyt, and K_{338}R, K_{346}R or KKRR mutants stably expressed in HeLa cells. Gray shading represents cells stained with a control antibody.

(C) Ubiquitination profile of WT or mutant TIM-1 was monitored with the FK2 antibody.

(D) Proximity ligation assay (Duolink) was performed in parental, TIM-1 WT, TIM-1 Δcyt-, or TIM-1 KKRR-expressing HeLa cells using goat anti-TIM-1 and mouse FK2 antibodies. Positive interactions between ubiquitin and the TIM-1 receptor are represented by red spots. Images are representative of two independent experiments. Scale bars, 10 μm.

(E) Parental or TIM-1 mutant-expressing HeLa cells were challenged with DENV2 JAM at the indicated MOIs. Infection was quantified 24 hpi by flow cytometry. Data are shown as mean ± SD of three independent experiments.

(F) Parental, TIM-1 WT, TIM-1Δcyt-, or TIM-1 KKRR-expressing HeLa cells were incubated with DENV2 for 1 hr on ice, shifted to 37°C for 2 hr, and treated with proteinase K for 45 min at 4°C to remove cell surface-bound particles. Internalized DENV viral RNA was quantified by qRT-PCR.

(G) Parental, TIM-1 WT, TIM-1Δcyt-, or TIM-1 KKRR-expressing HeLa cells were incubated with DENV2 AF594 for 1 hr on ice, shifted to 37°C for 30 min, or kept at 4°C as a control. Cell surface-bound particles were eliminated with trypsin treatment. DENV2 AF594-bound particles were quantified using Fiji software. Data shown are mean ± SD of at least three independent experiments (n > 150).

(H) Parental, TIM-1 WT, or TIM-1 KKRR HeLa cells were incubated on ice with DENV2 JAM at an MOI of 50. Cells were shifted to 37°C for 60 min and treated or not treated with trypsin for 15 min at 4°C. Cells were then fixed and stained for DENV viral RNA (red). White lines outline the cell membrane. Images are representative of at least three independent experiments (n > 30). Scale bars, 10 μm. Right: quantification of spot number per cell obtained from FISH images using ImageJ software.

(I) Fluorescent DENV2 AF594 particles were added to HeLa TIM-1 GFP, TIM-1Δcyt GFP, or TIM-1 KKRR GFP at 37°C. Cells were imaged by TIRF microscopy, and viral particles (spots) inside the yellow line were quantified over time using Fiji software from the different videos recorded. Yellow lines outline the edge of cells. Dot quantifications are representative of five independent experiments.

For (E)–(H), significance was calculated using one-way ANOVA; $^{**}p < 0.001$, $^{***}p < 0.0001$.

Table 1. A Subset of TIM-1-Associated Proteins Identified by SILAC Differential Proteomics

Protein Name	Number of Peptides	Molecular Weight (kDa)	SILAC Labeling (Ratio H/L)
TNFRSF10B	3	47.88	11.9
ACVR1B	2	56.81	9.83
DDR2	3	96.74	7.46
TGFBR1	20	55.96	6.7
NDFIP1	4	24.90	5.36
STUB1	2	34.86	4.44
ABCG2	8	72.31	4.42
SNX17	3	52.90	4.18
PI4K2A	5	51.02	4.03
UBA52	54	14.73	4.01
ATP1A1	207	112.90	3.56
SLC12A3	3	113.14	3.54
SNX6	4	46.65	3.24
ATP1B1	14	35.06	3.15
ITCH	3	102.80	3.12
FYN	7	60.76	3.11
STAM	3	59.18	2.62
TFRC	107	84.87	2.57
YWHAE	23	29.17	2.56
WWP2	3	98.91	2.44
DNAJA3	5	52.49	2.39
NEDD4L	3	111.93	2.36

HeLa TIM-1 and HeLa TIM-1 FLAG-HA cells were differentially labeled with the SILAC method. TIM-1-associated proteins were sequentially co-precipitated with FLAG and HA. The specificity threshold of TIM-1 association from individual identified protein was defined as a peak volume ratio H/L > 2 of the differentially isotope-labeled versions of each protein.

infection. We silenced the expression of each of these factors by RNAi and investigated their effect on DENV infection (Figure S6F). This RNAi screen identified UBA52, ITCH, and STAM-1 as TIM-1 partners required for DENV infection (Figure S6F). We focused our work on STAM-1, one of the two components of ESCRT-0 implicated in endosomal sorting of ubiquitinated receptors (Haglund and Dikic, 2012). STAM-1 interacts with TIM-1 WT but to a lesser extend with TIM Δcyt or TIM KKRR mutants (Figure 6A). We then stained STAM-1 by immunofluorescence and observed a marked co-localization with TIM-1 GFP in HeLa cells (Figure 6B). This suggested that TIM-1 traffics through STAM-1-positive endosomes. Moreover, silencing STAM-1 with small interfering RNA (siRNA) (Figure 6C) diminished TIM-1 cell surface expression (Figure 6D) and inhibited DENV binding and endocytosis (Figure 6E). Depletion of STAM-1 inhibited DENV infection in HeLa TIM-1 cells (Figure 6F) and in human cells that endogenously express TIM-1 (Figure 6G) without interfering with DENV translation and vRNA amplification (Figure S6G). Consistent with these data, we observed that silencing of HRS, a STAM-1 binding partner and component of the ESCRT-0 complex, significantly reduced DENV infection (Figure 6H).

In conclusion, our study brings insights into the cell biology of DENV entry. We provide several lines of evidence that TIM-1 is an authentic DENV receptor required for virus binding and endocytosis. Using a panel of complementary techniques, including live-imaging TIRF microscopy, we analyzed the dynamics of TIM-1-mediated entry of DENV. We propose that, when adsorbed on the cell surface, DENV diffuses at the plasma membrane until it reaches TIM-1 clusters, predominantly stuck in preexisting CCPs, where TIM-1/DENV complexes will be rapidly co-internalized. This is in agreement with previous reports showing that DENV enters a host cell by rolling on the plasma membrane to reach preexisting CCPs (van der Schaar et al., 2007, 2008). In contrast to entry of Ebola virus (Moller-Tank et al., 2014) or phagocytosis of apoptotic cells, DENV endocytosis relies on the TIM-1 cytoplasmic tail. Tail-less TIM-1 molecules have a defect in internalization and are unable to promote DENV uptake. We demonstrate for the first time that TIM-1 is ubiquitinated at K338 and K346 residues and that this post-translational modification is required for DENV entry. Ubiquitination is a well-known modification involved in the regulation of cell surface proteins by promoting internalization and sorting toward late endosome/lysosomes (Haglund and Dikic, 2012; Shih et al., 2000). It has been reported for EGFR that ligand binding promotes ubiquitination and alters trafficking (Sigismund et al., 2005). Because DENV predominantly fuses within late endosomes (Smit et al., 2011; van der Schaar et al., 2008), it is tempting to speculate that DENV binding to TIM-1 may stimulate sorting of the receptor to late endosomes. Consistent with a role of TIM-1 ubiquitination in DENV entry, our proteomics analysis of TIM-1 binding partners identified various component of the Ub machinery as well as STAM-1 as a new host factor required for DENV infection. Several PS receptors, including Axl and CD300a, have been identified as DENV entry factors (Carnec et al., 2015; Meertens et al., 2012) and might accomplish non-redundant functions during DENV infection. CD300a acts as a DENV binding molecule without promoting viral uptake (Carnec et al., 2015). Axl promotes DENV entry and also induces intracellular signaling that dampens innate immune responses and favors viral replication (Bhattacharyya et al., 2013; Chen et al., 2018; Meertens et al., 2012, 2017). It is thus likely that these different PS receptors play complementary roles during DENV entry. Moreover, we noticed that TIM-1 KO cells are sensitive, at low levels, to DENV infection, indicating that uncharacterized DENV receptor(s) remain to be identified.

We also report that TIM-1 is endogenously expressed in the epidermis, mostly, if not exclusively, by keratinocytes of the basal layer. Infection experiments of skin explants previously revealed the presence of DENV-infected cells in this basal layer (Limon-Flores et al., 2005). It is tempting to speculate that TIM-1 may serve as an early DENV receptor in the skin during mosquito bites and may play a role in virus transmission. Targeting TIM-1 with antibodies or small molecules may provide effective flavivirus antiviral agents by interfering with viral entry.

EXPERIMENTAL PROCEDURES

Cells Lines and Viruses

HeLa, HEK293T, 769P, A549, and Huh7.5 cells were maintained in DMEM (Life Technologies) supplemented with 10% fetal bovine serum (FBS), 1%

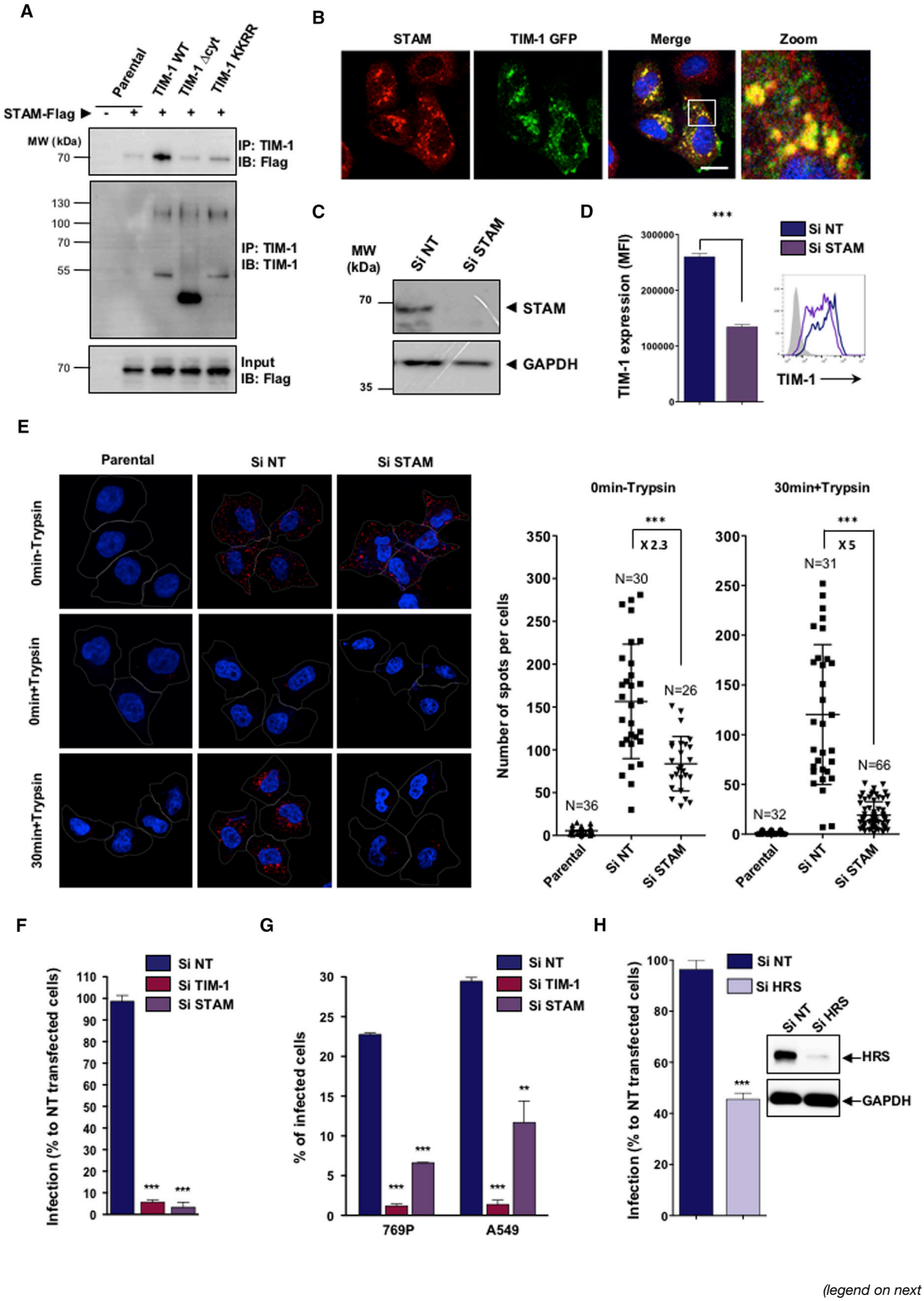

(legend on next page)

penicillin-streptomycin, and L-Glutamine (Life Technologies). Cells stably expressing TIM-1 or mutants were generated by transduction using pTRIP lentiviral vectors and sorted on a BD FACS Aria III (Becton Dickinson). DENV1 TVP5175, DENV2 JAM, DENV3 THAI, DENV4 1036, WNV, ZIKV HD78, and HSV-1 viruses were produced as described previously (Meertens et al., 2012).

Endocytosis Assay

Cells were grown on Lab-Tek chamber slides and incubated with mouse anti-TIM-1 (R&D Systems) primary Ab (30 μg/mL) with Tf Alexa Fluor A594-conjugated diluted at 1:50 (Life Technologies) or DENV2 AF594 at MOI 50 for 1 hr at 4°C. Cells were then washed with cold PBS and shifted to 37°C. At different time points, cells were fixed with PBS-paraformaldehyde (PFA) (4%) for 15 min at room temperature (RT) and then stained with a secondary Ab, goat anti-mouse Alexa Fluor 488, conjugated in the presence or absence of saponin (0.05%) to distinguished external and internalized receptors. Images were obtained by confocal microscopy (LSM700 Carl Zeiss, Jena).

Viral Internalization Assay

For immunofluorescence analysis, cells were seeded on Lab-Tek chamber slides (Nunc, Roskilde, Denmark). For qRT-PCR vRNA quantification, cells were seeded on 6-well plates. Cells were incubated with viral particles for 1 hr on ice, washed to remove unbound particles, and shifted to 37°C for 30 min or 2 hr. Cells were either treated or not with trypsin for 15 min or proteinase K (1 mg/mL) for 45 min on ice to remove non-internalized particles.

Live Microscopy and Data Analysis

For TIRF microscopy, cells were seeded on MatTek dishes (MatTek) and live cells were imaged with a Zeiss LSM780 Elyra TIRF microscope using ZEN software. For clathrin imaging, TIM-1 GFP cells were transfected for 48 hr with a plasmid expressing CLC-dsRed before imaging. For monitoring DENV2 AF594 internalization, TIM-1 GFP, TIM-1 Δcyt GFP, or TIM-1 KKRR GFP were imaged in the continuous presence of DENV2 AF594 at 37°C. Trajectories and fluorescence intensities of TIM-1 GFP and DENV2 AF594 spots were analyzed by computational analysis with TrackMate (Tinevez et al., 2017) and MATLAB (MathWorks). Quantification of DENV2 AF594 spots was assessed using Fiji software.

For live-cell confocal microscopy, cells were seeded on MatTek dishes, and images were acquired for 20 min at 1 image per 2 s on a spinning disk microscope (UltraVIEW VOX, PerkinElmer) in the continuous presence of DENV2 AF594. Quantification was assessed using Fiji software.

Transmission Electron Microscopy

For standard transmission electron microscopy, cells were scraped and fixed by incubation for 24 hr in 4% PFA and 1% glutaraldehyde (Sigma, St. Louis, MO) in 0.1 M phosphate buffer (pH 7.2). Samples were then washed in PBS and post-fixed by incubation with 2% osmium tetroxide (Agar Scientific, Stansted, UK) for 1 hr. Samples were then fully dehydrated in a graded series of ethanol solutions and propylene oxide. The impregnation step was performed with a mixture of (1:1) propylene oxide/Epon resin (Sigma) and then left overnight in pure resin. Cells were then embedded in Epon resin (Sigma), which was allowed to polymerize for 48 hr at 60°C. Ultra-thin sections (90 nm) of these blocks were obtained with an EM UC7 ultramicrotome (Leica Microsystems, Wetzlar, Germany). Sections were stained with 2% uranyl acetate (Agar Scientific) and 5% lead citrate (Sigma), and observations were made with a transmission electron microscope (JEOL 1011, Tokyo, Japan).

Immunogold Labeling of Cryosections According to the Tokuyasu Method for Immunoelectron Microscopy

Cells were fixed for 2 hr with 4% PFA in phosphate buffer (pH 7.6), washed with PBS (pH 7.6) twice for 5 min each time, and centrifuged at 300 × *g* for 10 min. After removing the supernatant, cell pellets were included in gelatin (12%) and infused with sucrose (2.3 M) overnight at 4°C. 90-nm ultra-thin cryosections were made at −110°C on a Leica Microsystems FC7 cryo-ultramicrotome. Sections were retrieved with a methylcellulose (2%)/sucrose (2.3 M) mixture (1:1) and collected onto formvar/carbon-coated nickel grids. After removal of gelatin at 37°C, sections were incubated with PBS containing 1:100 anti-TIM-1 and 1:100 anti-DENV. After six washes of PBS (5 min each), the grids were incubated with PBS containing 1:30 gold-conjugated goat-anti-mouse (6 nm) and 1:30 goat-anti-rabbit IgG (10 nm) (Aurion, Wageningen, the Netherlands). The grids were finally washed in PBS (six washes of 5 min each), post-fixed in 1% glutaraldehyde, and rinsed with distilled water. The contrasting step was performed by incubating grids in a 2% uranyl acetate/2% methylcellulose mixture (1:10). The sections were imaged with a transmission electron microscope at 100 kV (JEOL 1011).

Statistical Analysis

Graphical representation and statistical analyses were performed using Prism5 software (GraphPad). Unless otherwise stated, results are shown as means ± SD from three independent experiments. Differences were tested for statistical relevance using unpaired two-tailed t test or one-way ANOVA with Tukey post-test. Pierson correlation coefficient (PCC) was calculated using the ImageJ plugin Coloc2 and is represented as the mean ± SEM.

SUPPLEMENTAL INFORMATION

Supplemental Information includes Supplemental Experimental Procedures and six figures and can be found with this article online at https://doi.org/10.1016/j.celrep.2018.04.013.

ACKNOWLEDGMENTS

This study has received funding from the French government's Investissement d'Avenir program, Laboratoire d'Excellence "Integrative Biology of Emerging Infectious Diseases" (grant ANR-10-LABX-62-IBEID), and the CHIKV-Viro-Immuno ANR-14-CE14-0015-01 and TIMTAMDEN ANR-14-CE14-0029 projects. O.D and M.L.H are funded by fellowships from the Fondation pour la Recherche Médicale and ANR, respectively. The authors thank Dr. Alessia

Figure 6. STAM Interacts with TIM-1 and Is Important for DENV Infection

(A) Parental or HeLa cells expressing TIM-1 WT, Δcyt, or KKRR were transiently transfected with either a control or a STAM-FLAG-expressing plasmid. Cell lysates were subjected to immunoprecipitation (IP) using goat anti-TIM-1 antibody. The interaction between TIM-1 and STAM was revealed by immunoblot analysis using mouse anti-FLAG M2 antibody.

(B) Confocal microscopy images of TIM-1 GFP and endogenous STAM in fixed cells. Images are representative of at least three independent experiments. PCC, 0.605 ± 0.06. Scale bar, 10 μm.

(C) Validation of STAM protein knockdown by immunoblot analysis.

(D) HeLa TIM-1 cells transfected with siRNA NT (blue) or targeting STAM (purple) were analyzed for TIM-1 expression by flow cytometry. Gray shading represents cells stained with a control Ab.

(E) Parental or TIM-1 HeLa cells were transfected with the indicated siRNA. Cells were incubated with DENV2 JAM at an MOI of 50 at 37°C for 60 min and treated or not treated with trypsin. Cells were then fixed and stained for DENV viral RNA (red). White lines outline the cell membrane. Images are representative of at least three independent experiments (n > 30). Scale bar, 10 μm. Right: quantification of spot number per cell obtained from FISH images using ImageJ software.

(F and G) HeLa TIM-1 cells (F) or the 769P and A549 cell lines (G) were transfected with siRNA NT or targeting TIM-1 or STAM for 48 hr and challenged with DENV2 JAM. The percentage of infected cells was assessed 24 hpi using 2H2 antibody.

(H) HeLa TIM-1 cells were transfected with siRNA NT or targeting Hrs and analyzed as described in (F) and (G).

Data are shown as mean ± SD of at least two independent experiments. For (D)–(H), significance was calculated using one-way ANOVA and Tukey post-test (**p < 0.001, ***p < 0.0001).

Zamborlini for critical reading of the manuscript and Audrey Salles for help with TIRF microscopy experiments. We are most grateful to Dr. Daniel Aberdam for providing human skin explants.

AUTHOR CONTRIBUTIONS

Conceptualization, O.D., M.L.H., L.M., and A.A.; Investigation, O.D., M.L.H., M.C., M.V.., J.G., L.B.-M., X.C., M.P.-L., C.U.-D., J.-Y.T., C.D. and L.M; Writing – Original Draft, O.D., M.L.H., L.M., O.S., N.J., P.R., C.B.-T., and A.A.; Writing – Review & Editing, O.D., M.L.H., L.M., C.D., O.S., P.R., N.J., C.B.-T., and A.A.; Visualization, O.D., M.L.H., L.M., and A.A., Funding Acquisition, A.A. and O.S.

DECLARATION OF INTERESTS

The authors declare no competing interests.

Received: September 8, 2017
Revised: March 6, 2018
Accepted: April 2, 2018
Published: May 8, 2018

REFERENCES

Acosta, E.G., Castilla, V., and Damonte, E.B. (2008). Functional entry of dengue virus into Aedes albopictus mosquito cells is dependent on clathrin-mediated endocytosis. J. Gen. Virol. *89*, 474–484.

Acosta, E.G., Castilla, V., and Damonte, E.B. (2009). Alternative infectious entry pathways for dengue virus serotypes into mammalian cells. Cell. Microbiol. *11*, 1533–1549.

Amara, A., and Mercer, J. (2015). Viral apoptotic mimicry. Nat. Rev. Microbiol. *13*, 461–469.

Balasubramanian, S., Kota, S.K., Kuchroo, V.K., Humphreys, B.D., and Strom, T.B. (2012). TIM family proteins promote the lysosomal degradation of the nuclear receptor NUR77. Sci. Signal. *5*, ra90.

Bhatt, S., Gething, P.W., Brady, O.J., Messina, J.P., Farlow, A.W., Moyes, C.L., Drake, J.M., Brownstein, J.S., Hoen, A.G., Sankoh, O., et al. (2013). The global distribution and burden of dengue. Nature *496*, 504–507.

Bhattacharyya, S., Zagórska, A., Lew, E.D., Shrestha, B., Rothlin, C.V., Naughton, J., Diamond, M.S., Lemke, G., and Young, J.A. (2013). Enveloped viruses disable innate immune responses in dendritic cells by direct activation of TAM receptors. Cell Host Microbe *14*, 136–147.

Carnec, X., Meertens, L., Dejarnac, O., Perera-Lecoin, M., Hafirassou, M.L., Kitaura, J., Ramdasi, R., Schwartz, O., and Amara, A. (2015). The Phosphatidylserine and Phosphatidylethanolamine Receptor CD300a Binds Dengue Virus and Enhances Infection. J. Virol. *90*, 92–102.

Chen, Y., Maguire, T., Hileman, R.E., Fromm, J.R., Esko, J.D., Linhardt, R.J., and Marks, R.M. (1997). Dengue virus infectivity depends on envelope protein binding to target cell heparan sulfate. Nat. Med. *3*, 866–871.

Chen, J., Yang, Y.F., Yang, Y., Zou, P., Chen, J., He, Y., Shui, S.L., Cui, Y.R., Bai, R., Liang, Y.J., et al. (2018). AXL promotes Zika virus infection in astrocytes by antagonizing type I interferon signalling. Nat. Microbiol. *3*, 302–309.

Curtiss, M.L., Hostager, B.S., Stepniak, E., Singh, M., Manhica, N., Knisz, J., Traver, G., Rennert, P.D., Colgan, J.D., and Rothman, P.B. (2011). Fyn binds to and phosphorylates T cell immunoglobulin and mucin domain-1 (Tim-1). Mol. Immunol. *48*, 1424–1431.

Freeman, G.J., Casasnovas, J.M., Umetsu, D.T., and DeKruyff, R.H. (2010). TIM genes: a family of cell surface phosphatidylserine receptors that regulate innate and adaptive immunity. Immunol. Rev. *235*, 172–189.

Guzman, M.G., and Harris, E. (2015). Dengue. Lancet *385*, 453–465.

Haglund, K., and Dikic, I. (2012). The role of ubiquitylation in receptor endocytosis and endosomal sorting. J. Cell Sci. *125*, 265–275.

Hamel, R., Dejarnac, O., Wichit, S., Ekchariyawat, P., Neyret, A., Luplertlop, N., Perera-Lecoin, M., Surasombatpattana, P., Talignani, L., Thomas, F., et al. (2015). Biology of Zika Virus Infection in Human Skin Cells. J. Virol. *89*, 8880–8896.

Jemielity, S., Wang, J.J., Chan, Y.K., Ahmed, A.A., Li, W., Monahan, S., Bu, X., Farzan, M., Freeman, G.J., Umetsu, D.T., et al. (2013). TIM-family proteins promote infection of multiple enveloped viruses through virion-associated phosphatidylserine. PLoS Pathog. *9*, e1003232.

Kobayashi, N., Karisola, P., Peña-Cruz, V., Dorfman, D.M., Jinushi, M., Umetsu, S.E., Butte, M.J., Nagumo, H., Chernova, I., Zhu, B., et al. (2007). TIM-1 and TIM-4 glycoproteins bind phosphatidylserine and mediate uptake of apoptotic cells. Immunity *27*, 927–940.

Kondratowicz, A.S., Lennemann, N.J., Sinn, P.L., Davey, R.A., Hunt, C.L., Moller-Tank, S., Meyerholz, D.K., Rennert, P., Mullins, R.F., Brindley, M., et al. (2011). T-cell immunoglobulin and mucin domain 1 (TIM-1) is a receptor for Zaire Ebolavirus and Lake Victoria Marburgvirus. Proc. Natl. Acad. Sci. USA *108*, 8426–8431.

Kuhn, R.J., Zhang, W., Rossmann, M.G., Pletnev, S.V., Corver, J., Lenches, E., Jones, C.T., Mukhopadhyay, S., Chipman, P.R., Strauss, E.G., et al. (2002). Structure of dengue virus: implications for flavivirus organization, maturation, and fusion. Cell *108*, 717–725.

Lemke, G., and Rothlin, C.V. (2008). Immunobiology of the TAM receptors. Nat. Rev. Immunol. *8*, 327–336.

Leventis, P.A., and Grinstein, S. (2010). The distribution and function of phosphatidylserine in cellular membranes. Annu. Rev. Biophys. *39*, 407–427.

Limon-Flores, A.Y., Perez-Tapia, M., Estrada-Garcia, I., Vaughan, G., Escobar-Gutierrez, A., Calderon-Amador, J., Herrera-Rodriguez, S.E., Brizuela-Garcia, A., Heras-Chavarria, M., Flores-Langarica, A., et al. (2005). Dengue virus inoculation to human skin explants: an effective approach to assess in situ the early infection and the effects on cutaneous dendritic cells. Int. J. Exp. Pathol. *86*, 323–334.

Lozach, P.Y., Burleigh, L., Staropoli, I., Navarro-Sanchez, E., Harriague, J., Virelizier, J.L., Rey, F.A., Desprès, P., Arenzana-Seisdedos, F., and Amara, A. (2005). Dendritic cell-specific intercellular adhesion molecule 3-grabbing non-integrin (DC-SIGN)-mediated enhancement of dengue virus infection is independent of DC-SIGN internalization signals. J. Biol. Chem. *280*, 23698–23708.

Meertens, L., Carnec, X., Lecoin, M.P., Ramdasi, R., Guivel-Benhassine, F., Lew, E., Lemke, G., Schwartz, O., and Amara, A. (2012). The TIM and TAM families of phosphatidylserine receptors mediate dengue virus entry. Cell Host Microbe *12*, 544–557.

Meertens, L., Labeau, A., Dejarnac, O., Cipriani, S., Sinigaglia, L., Bonnet-Madin, L., Le Charpentier, T., Hafirassou, M.L., Zamborlini, A., Cao-Lormeau, V.M., et al. (2017). Axl Mediates ZIKA Virus Entry in Human Glial Cells and Modulates Innate Immune Responses. Cell Rep. *18*, 324–333.

Mercer, J., and Helenius, A. (2008). Vaccinia virus uses macropinocytosis and apoptotic mimicry to enter host cells. Science *320*, 531–535.

Moller-Tank, S., Kondratowicz, A.S., Davey, R.A., Rennert, P.D., and Maury, W. (2013). Role of the phosphatidylserine receptor TIM-1 in enveloped-virus entry. J. Virol. *87*, 8327–8341.

Moller-Tank, S., Albritton, L.M., Rennert, P.D., and Maury, W. (2014). Characterizing functional domains for TIM-mediated enveloped virus entry. J. Virol. *88*, 6702–6713.

Morizono, K., and Chen, I.S. (2014). Role of phosphatidylserine receptors in enveloped virus infection. J. Virol. *88*, 4275–4290.

Navarro-Sanchez, E., Altmeyer, R., Amara, A., Schwartz, O., Fieschi, F., Virelizier, J.L., Arenzana-Seisdedos, F., and Desprès, P. (2003). Dendritic-cell-specific ICAM3-grabbing non-integrin is essential for the productive infection of human dendritic cells by mosquito-cell-derived dengue viruses. EMBO Rep. *4*, 723–728.

Perera-Lecoin, M., Meertens, L., Carnec, X., and Amara, A. (2013). Flavivirus entry receptors: an update. Viruses *6*, 69–88.

Poulter, N.S., Pitkeathly, W.T., Smith, P.J., and Rappoport, J.Z. (2015). The physical basis of total internal reflection fluorescence (TIRF) microscopy and its cellular applications. Methods Mol. Biol. *1251*, 1–23.

Santiago, C., Ballesteros, A., Tami, C., Martínez-Muñoz, L., Kaplan, G.G., and Casasnovas, J.M. (2007). Structures of T Cell immunoglobulin mucin receptors 1 and 2 reveal mechanisms for regulation of immune responses by the TIM receptor family. Immunity *26*, 299–310.

Shih, S.C., Sloper-Mould, K.E., and Hicke, L. (2000). Monoubiquitin carries a novel internalization signal that is appended to activated receptors. EMBO J. *19*, 187–198.

Shimojima, M., Takada, A., Ebihara, H., Neumann, G., Fujioka, K., Irimura, T., Jones, S., Feldmann, H., and Kawaoka, Y. (2006). Tyro3 family-mediated cell entry of Ebola and Marburg viruses. J. Virol. *80*, 10109–10116.

Sigismund, S., Woelk, T., Puri, C., Maspero, E., Tacchetti, C., Transidico, P., Di Fiore, P.P., and Polo, S. (2005). Clathrin-independent endocytosis of ubiquitinated cargos. Proc. Natl. Acad. Sci. USA *102*, 2760–2765.

Simhadri, V.R., Andersen, J.F., Calvo, E., Choi, S.C., Coligan, J.E., and Borrego, F. (2012). Human CD300a binds to phosphatidylethanolamine and phosphatidylserine, and modulates the phagocytosis of dead cells. Blood *119*, 2799–2809.

Smit, J.M., Moesker, B., Rodenhuis-Zybert, I., and Wilschut, J. (2011). Flavivirus cell entry and membrane fusion. Viruses *3*, 160–171.

Stiasny, K., Fritz, R., Pangerl, K., and Heinz, F.X. (2011). Molecular mechanisms of flavivirus membrane fusion. Amino Acids *41*, 1159–1163.

Tassaneetrithep, B., Burgess, T.H., Granelli-Piperno, A., Trumpfheller, C., Finke, J., Sun, W., Eller, M.A., Pattanapanyasat, K., Sarasombath, S., Birx, D.L., et al. (2003). DC-SIGN (CD209) mediates dengue virus infection of human dendritic cells. J. Exp. Med. *197*, 823–829.

Tinevez, J.Y., Perry, N., Schindelin, J., Hoopes, G.M., Reynolds, G.D., Laplantine, E., Bednarek, S.Y., Shorte, S.L., and Eliceiri, K.W. (2017). TrackMate: An open and extensible platform for single-particle tracking. Methods *115*, 80–90.

van der Schaar, H.M., Rust, M.J., Waarts, B.L., van der Ende-Metselaar, H., Kuhn, R.J., Wilschut, J., Zhuang, X., and Smit, J.M. (2007). Characterization of the early events in dengue virus cell entry by biochemical assays and single-virus tracking. J. Virol. *81*, 12019–12028.

van der Schaar, H.M., Rust, M.J., Chen, C., van der Ende-Metselaar, H., Wilschut, J., Zhuang, X., and Smit, J.M. (2008). Dissecting the cell entry pathway of dengue virus by single-particle tracking in living cells. PLoS Pathog. *4*, e1000244.

Vanlandschoot, P., and Leroux-Roels, G. (2003). Viral apoptotic mimicry: an immune evasion strategy developed by the hepatitis B virus? Trends Immunol. *24*, 144–147.